ACS APPLIED MATERIALS & INTERFACES

www.acsami.org

Research Article

Superhydrophilic Modification of Polyvinylidene Fluoride Membrane via a Highly Compatible Covalent Organic Framework−COOH/Dopamine-Integrated Hierarchical Assembly Strategy for Oil−Water Separation

Qi Liang, Bin Jiang, Na Yang, Longfei Zhang, Yongli Sun, and Luhong Zhang*

Cite This: *ACS Appl. Mater. Interfaces* 2022, 14, 45880−45892

Read Online

ACCESS | Metrics & More | Article Recommendations | Supporting Information

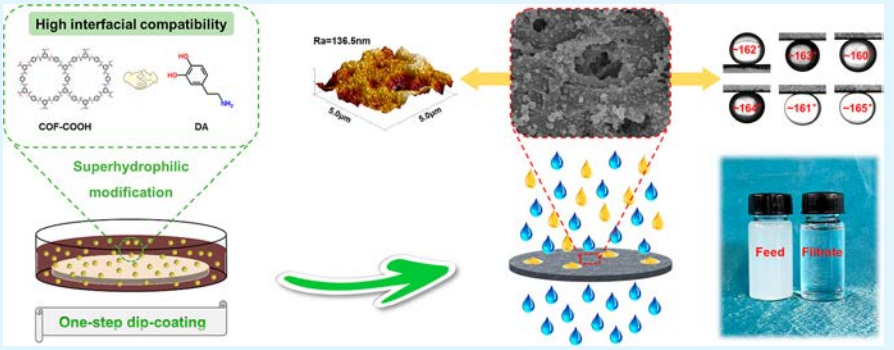

ABSTRACT: The integration of membranes with additives such as functionalized nanomaterials can be recognized as an effective method to enhance membrane performance. However, to obtain an efficient nanoparticle-decorated membrane, the compatibility of nanomaterials remains a challenge. Hydrophilic carboxylated covalent organic frameworks (COF−COOH) might be expected to avoid the drawbacks of aggregation and easy shedding of inorganic materials caused by the poor interfacial compatibility. Herein, a highly compatible dip-coating strategy was proposed for the superhydrophilic modification of polyvinylidene fluoride membrane via COF−COOH integrated with dopamine. COF−COOH together with polydopamine nanoparticles were uniformly and stably attached to the membrane due to the high interfacial compatibility, constructing a coating with rough hierarchical nanostructures and abundant carboxyl groups. The synergistic effects of multiscale structures and chemical groups endow the membrane with superhydrophilicity and underwater superoleophobicity, the water contact angle decreased from 123 to 15°, and the underwater oil contact angle increased from 132 to 162°. Accordingly, the modified membrane exhibits an ultrahigh oil rejection ratio (>98%), a high flux (the maximum reaches 1843.48 L m^{-2} h^{-1} bar^{-1}), attractive antifouling ability, and impregnable stability. This work would provide a momentous reference for the application of COF−COOH in practical oily wastewater treatment.

KEYWORDS: *superhydrophilic, interfacial compatibility, carboxylated covalent organic frameworks, hierarchical nanostructures, oil−water separation*

1. INTRODUCTION

In recent decades, with the accelerated evolution of industry and the intensifying human activities, the excessive discharge of oily wastewater has not only seriously damaged the ecological environment but also wasted plentiful precious resources.[1−4] For oily wastewater, especially the emulsified one, it is necessary to be treated and purified before being released into the ecosystem. Currently, several approaches such as air flotation,[5] gravity sedimentation,[6] chemical coagulation,[7] adsorption,[8] and centrifugation[9] have been adopted for oil−water separation. However, these traditional treatment technologies always have the disadvantages of secondary pollution, low separation efficiency, and high energy consumption.[10−13] In recent years, microfiltration and ultrafiltration polymer membranes have shown unique performance in oil−water separation and are suitable for separating the emulsified oily wastewater with high stability and relatively small droplet size (<20 μm), which is difficult to be treated by traditional methods.[14−16] Polyvinylidene fluoride (PVDF) membrane, as one of the most common porous polymer membranes, has been widely applied in the

Received: July 26, 2022
Accepted: September 14, 2022
Published: September 27, 2022

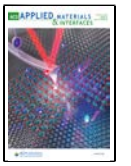

Scheme 1. Schematic Diagram of the (a) Chemical Reaction Process and the Periodical Order Structure of COF−COOH, (b) Preparation Process of Coating Solutions, and (c) Modification of the PVDF Membrane

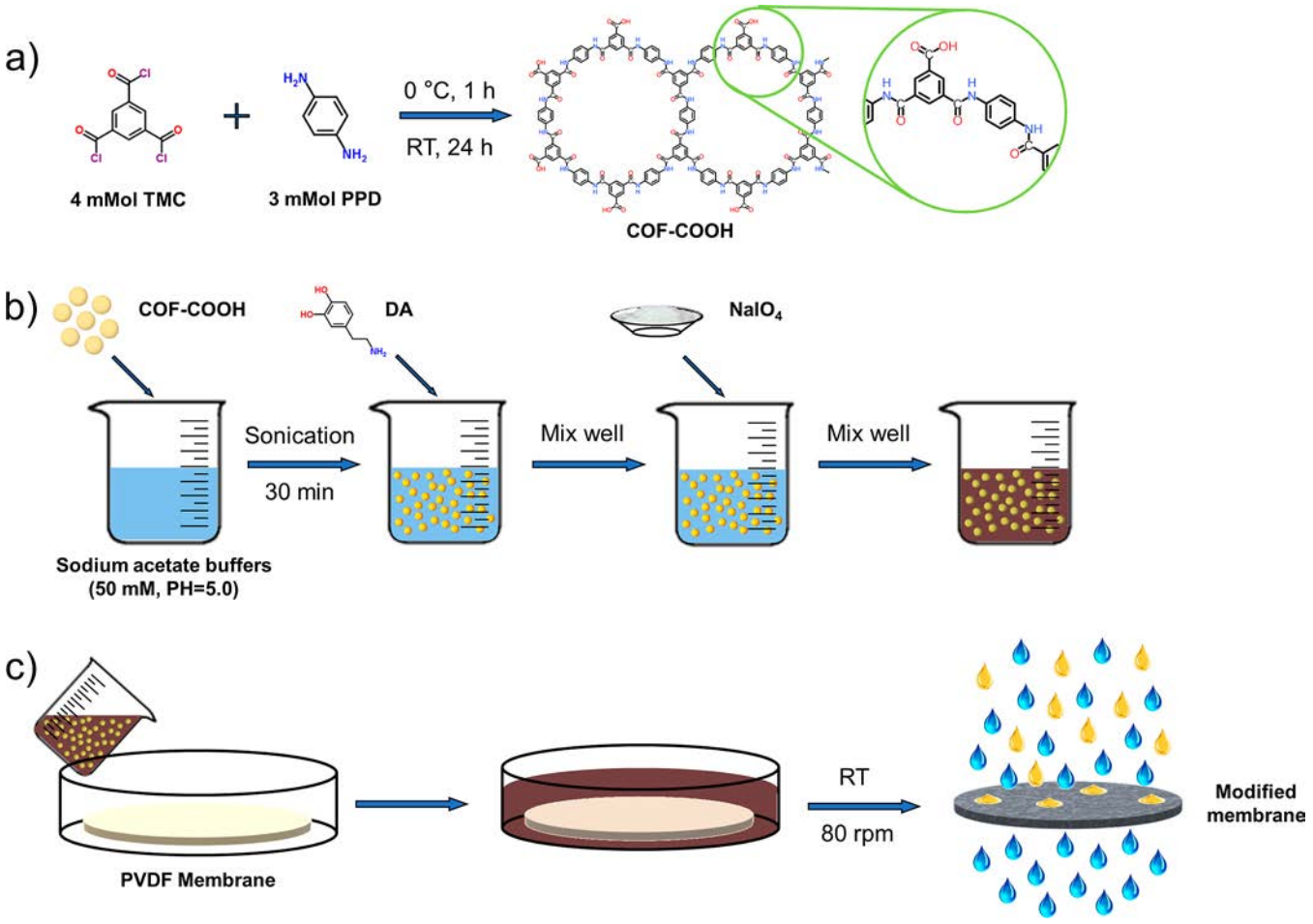

separation of oil-in-water emulsions due to its high mechanical strength and excellent stability.[17−20] However, membrane fouling commonly exists due to the intrinsic hydrophobicity of PVDF and the strong adhesion property of oil droplets, which seriously affects the filtration efficiency and working longevity of the membrane.[21,22] Thus, reducing membrane fouling is critical to maintaining long-term efficient separation during the treatment of oily wastewater.

Hydrophilic modification of the hydrophobic membrane has been probed as a helpful way to improve the antifouling ability to reduce the oil adhesion on the surface.[23−25] The polydopamine (PDA) hydrophilic coating formed by oxidative self-polymerization of dopamine (DA) can adhere firmly to the surface of various materials, which provides a versatile strategy for hydrophilic modification.[26,27] However, the coatings equipped only by PDA are always arduous to satisfy the demands of efficient oil−water separation by reason of their limited hydrophilicity. It is noteworthy that the hydrophilicity of the membrane can be intensified by increasing the surface roughness according to the capillary effect proved by Wenzel mode.[28] For example, some inorganic nanomaterials such as SiO_2 and TiO_2 were successfully incorporated with PVDF membranes via the self-polymerization of DA. The special surface micro−nano structure appearing on the modified membranes greatly enhanced the hydrophilicity by improving the surface roughness.[29,30] Nonetheless, there are still some disadvantages of uneven distribution, clog channels, poor stability, and easy shedding caused by the poor interfacial compatibility of inorganic nanoparticles with the system. Besides, some metal−organic frameworks such as ZIF-8 and UiO-66 have also been applied in hydrophilic modification for efficient oil−water separation but are accompanied by additional complex and time-consuming modification procedures due to their inherent hydrophobicity.[31,32] Therefore, integrating hydrophilic-functionalized organic nanomaterials with high interfacial compatibility is promising to avert the above drawbacks.

Covalent organic frameworks (COFs) are considered as promising polymers because of their advantages of low mass densities, high porosity, high specific surface area, and great stability.[33,34] Recently, COFs have attracted extensive attention in the fields of dye separation,[35] desalination,[36] and oil−water separation.[37] The current research on the application of COFs in oil−water separation mainly focuses on superhydrophobic modification, which display the advantages of high surface roughness, outstanding stability, and excellent separation efficiency. However, the superhydrophobic modification of COFs by fluorinated chemicals greatly increases the cost,[37−40] and the preparation of most hydrophobic COFs is complicated, time-consuming, and under harsh reaction conditions.[41,42] Thus, the development of inexpensive raw materials, simple preparation processes, as well as hydrophilic modification methods might be the focus of COFs applied in oil−water separation in future research. To the best of our knowledge, hydrophilic modification using COFs for oil−water separation

https://doi.org/10.1021/acsami.2c13402
ACS Appl. Mater. Interfaces 2022, 14, 45880−45892

needs to be studied. Recently, the COF−COOH simply synthesized from trimesoyl chloride (TMC) and *p*-phenylenediamine (PPD) has shown excellent hydrophilicity due to its abundant carboxyl groups.[43] The development of COF−COOH makes it possible to use COFs for superhydrophilic modification of membrane to separate oil-in-water emulsions. In addition, introducing COF−COOH on the membrane not only improves the roughness to further strengthen the hydrophilicity but also enhances the surface electronegativity to provide a stronger repulsion to negatively charged oil droplets.[44] Furthermore, COF−COOH and PDA coatings exhibit splendid interfacial compatibility because of their similar chemical structure.[45,46]

In this paper, we conceived a facile hierarchical assembly strategy to assemble COF−COOH onto intrinsic hydrophobic PVDF membrane via PDA one-step dip-coating method. Considering the long deposition time of PDA in a conventional environment,[47,48] a slightly acidic oxidation system of sodium periodate ($NaIO_4$) was used to shorten the membrane modification time.[49,50] Due to the high interfacial compatibility, COF−COOH was uniformly deposited on the surface and pore channels of the membrane, forming a coating with rough hierarchical nanostructures and abundant carboxyl groups. The synergistic effects of the multiscale surface structure together with chemical functional groups greatly upgraded the membrane superhydrophilicity, resulting in an impregnable oil-repellent hydration layer and exceptional oil−water separation performance. Next, the effects of the coating time as well as the amount of COF−COOH on membrane penetrability and wettability were systematically studied. Furthermore, the separation performance, anti-oil fouling property, reusability, and stability of the modified membrane were evaluated comprehensively. The strategy proposed in this research may offer more possibilities for the application of hydrophilic-functionalized COF−COOH.

2. EXPERIMENTAL SECTION

2.1. Materials. Hydrophobic PVDF microfiltration (0.1 μm) membranes were bought from Haining Zhongli Filtration Co., Ltd. TMC (AR), dopamine hydrochloride (DA·HCl, 98%), PPD (AR), $NaIO_4$ (AR), ethyl acetate (EA, AR), and ethanol (EtOH, AR) were supplied by Shanghai Aladdin Chemicals Co., Ltd. Sodium acetate (0.1 M, pH = 5.0) buffers and oil red O were purchased from Nanjing SenBeiJia biological technology Co., Ltd. Sodium dodecyl sulfate (SDS, AR), *n*-hexane (AR), petroleum ether (PE, AR), and dichloromethane (DCM, AR) were bought from Tianjin Kermel reagents Co., Ltd. Diesel oil was obtained from China Petroleum and Chemical Corporation Tianjin Branch. Soybean oil was purchased from Beijing COFCO, China. Kerosene was supplied by Tianjin Yuanli Chemical Reagent Company. Deionized (DI) water was used for all experiments in this study.

2.2. Preparation of COF−COOH. COF−COOH was prepared according to the procedures described in the literature.[45] The corresponding chemical reaction is shown in Scheme 1a. Specifically, 4 mmol TMC (1.06 g)/30 mL EA solution was added to a round-bottom flask (100 mL), followed by dropwise addition of 3 mmol PPD (0.32 g)/15 mL EA solution with stirring at 0 °C. The yellowish solid sample was obtained by reacting for 24 h at room temperature. After being separated by centrifugation, the product was fully rinsed with DI water, EtOH, and acetone separately. Finally, the COF−COOH was dried under vacuum for 12 h at 55 °C and stored until use.

2.3. Superhydrophilic Modification of PVDF Membrane. The preparation process of the coating solution is shown in Scheme 1b. A certain amount of COF−COOH was added into 50 mL of sodium acetate buffer solution (50 mM, pH = 5.0) and sonicated for 30 min to ensure good dispersion of nanoparticles. Then, DA was added and stirred to dissolve, followed by $NaIO_4$ (4 mg/mL). After stirring evenly, the coating solution was obtained. Before hydrophilic modification, the PVDF membranes were rinsed with EtOH and DI water sequentially to remove residuals and impurities. The modification process of the membrane is shown in Scheme 1c. The treated membranes were immersed into the coating solution and shaken on a shaker with a fixed rate of 80 rpm at room temperature. The modified membranes were obtained after thorough washing with DI water and denoted as COF_X/DA_Y-Z, where *X* and *Y* refer to the content of COF−COOH (*X* mg/mL) and DA (*Y* mg/mL) in the coating solution, respectively, and *Z* represents the coating time (*Z* h). Table S1 lists the modification conditions and abbreviations of all membranes involved in this study. Prior to various characterizations and tests, the modified membranes were dried for 6 h at 40 °C.

2.4. Characterization. Scanning electron microscopy (SEM, Hitachi, S-4800, Japan) was used to observe the microscopic morphology of COF−COOH and the surface morphology of the membranes. Fourier transform infrared (FTIR) spectroscopy (Bruker, TENSOR 27, Germany) and attenuated total reflectance FTIR spectroscopy (ATR−FTIR, Bruker, TENSOR II, Germany) were applied to measure the chemical compositions of COF−COOH and the membrane surface, respectively. X-ray photoelectron spectroscopy (XPS, Thermo ESCALAB 250Xi, US) was used to determine the elemental compositions (mainly C, N, O, and F) of the membranes. An electro-kinetic analyzer (SF-SA, Saifei, China) was applied to measure the surface charge (zeta potential) of membranes based on the streaming potential method at a fixed pH of 7.0. Atomic force microscopy (AFM, Bruker, Multimode 8, Germany) was used to characterize the surface roughness of the membranes. A JC 2000 goniometer (Powereach, China) was used to measure the water contact angle (WCA) and underwater oil contact angle (UOCA) of membranes, and the volumes of the water droplet and oil droplet were 2 and 3 μL, respectively. Besides, a total organic carbon analyzer (Shimadzu, Japan) was applied to determine the oil concentrations in the feed and filtrate of oil-in-water emulsions.

2.5. Separation Performance of Membranes. To obtain various oil-in-water emulsions, 0.1 g of SDS and 1 g of pure oil (diesel oil, *n*-hexane, soybean oil, kerosene, and PE, respectively) were added to 1000 mL of DI water and dispersed in a homogenizer (FLUKO FA25, Germany) at 10,000 rpm for 30 min. The permeation test was performed through a cross-flow apparatus with an effective filtration area of 7.07 cm^2 as shown in Figure S1. The oil-in-water emulsion separation experiment for each dry membrane was carried out at a transmembrane pressure of 0.5 bar. The filtrate within the first 4 min was collected on account of the decrease in flux resulting from the gradually formed oil cake. The flux and the oil rejection ratio (*R*) were determined by eqs 1 and 2, respectively

$$\text{Flux} = \frac{V}{A \cdot \Delta t \cdot \Delta P} \tag{1}$$

where *V* represents the filtrate volume (L), *A* attributes to the effective filtration area (m^2), Δt corresponds to the separation time (h), and ΔP refers to the transmembrane pressure (bar).

$$R = \left(1 - \frac{C_p}{C_f}\right) \times 100\% \tag{2}$$

where C_f and C_p correspond to the oil concentrations in the feed and permeate.

To study the deposited amount of hydrophilic coating, the weight gain percent (W_g) of the modified membrane was calculated by eq 3.[20]

$$W_g = \frac{W_m - W_p}{W_p} \times 100\% \tag{3}$$

where W_p (g) and W_m (g) refer to the weight of the pristine PVDF membrane and the modified membrane, respectively.

Additionally, to further investigate the practical application ability of the membrane developed in this work, the real oily wastewater samples were analogously prepared by the river water obtained from the Haihe

https://doi.org/10.1021/acsami.2c13402
ACS Appl. Mater. Interfaces 2022, 14, 45880−45892

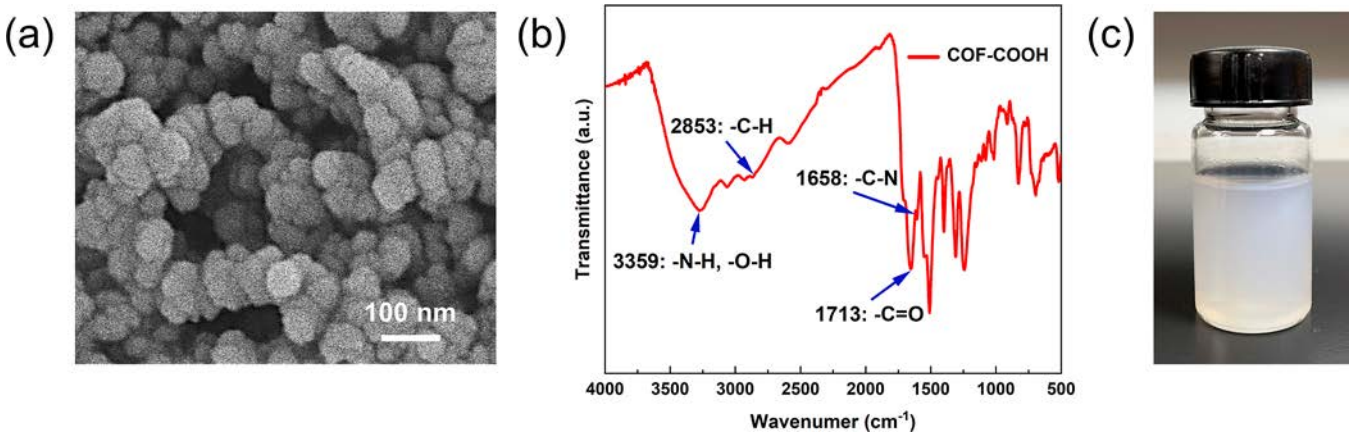

Figure 1. (a) SEM image and (b) FTIR spectrum of COF−COOH. (c) Dispersion of COF−COOH in sodium acetate (1 M, pH = 5.0) buffers.

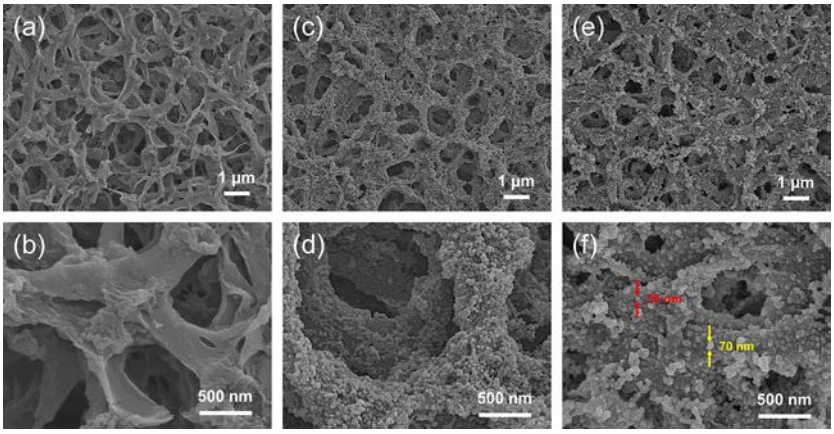

Figure 2. SEM images of (a,b) pristine PVDF membrane, (c,d) COF_0/DA_2-2, and (e,f) $COF_{0.2}/DA_2$-2.

River and used to test the flux and oil rejection ratio of the membrane. The preparation method is the same as the above-mentioned oil-in-water emulsions (DI water was replaced with the river water).

2.6. Antifouling Tests and Stability Tests. The antifouling property and reusability of the modified membrane were investigated through five-cycle filtration experiments on diesel-in-water emulsion. The real-time permeate flux was documented every 1 min within 10 min. Before the next experiment, the tested membrane was washed thoroughly by DI water to recover the permeate flux between two cycles. The oil rejection ratio was also determined during each filtration. Besides, the pure water flux of the tested membrane was measured before and after the five-cycle diesel-in-water emulsion filtration, and flux recovery ratio (FRR) was determined by eq 4

$$\mathrm{FRR} = \frac{J_w}{J_{w0}} \times 100\% \tag{4}$$

where J_w ($\mathrm{L\,m^{-2}\,h^{-1}\,bar^{-1}}$) and J_{w0} ($\mathrm{L\,m^{-2}\,h^{-1}\,bar^{-1}}$) represent the pure water flux of the tested membrane after the five-cycle emulsion separation experiments and the initial pure water flux, respectively.

The modified membrane samples were soaked in the solutions with different pH values (pH = 2, 7, and 12) for 12 h to investigate the chemical stability, and then the WCAs and UOCAs were measured and compared. The coating stability of the modified membrane was also tested. After each 1 min sonication treatment, the WCAs and UOCAs were determined. The procedure was repeated five times. Besides, to inspect the long-term stability of the modified membrane, long-term rinsing test was carried out. The modified membrane samples were immersed into DI water, then oscillated, and washed in a shaker with a fixed rate of 100 rpm at room temperature for 15 days. During the rinsing process, the WCAs and UOCAs were determined every 3 days.

3. RESULTS AND DISCUSSION

3.1. Characterization of COF−COOH. The COF−COOH was synthesized by amidation polymerization of TMC and PPD. The microscopic morphology was characterized by SEM, COF−COOH shows spherical particles of 65−75 nm in size as presented in Figure 1a. The chemical groups of COF−COOH were investigated by FTIR. As shown in Figure 1b, the strong characteristic peak at 1713 cm^{-1} represents −C═O in −COOH, indicating the abundant carboxyl groups of COF−COOH. The characteristic peak at 1658 cm^{-1} was attributed to −C−N demonstrating the amidation reaction of $-NH_2$ and −COCl. The −C−H stretching vibration of the aromatic structure caused the peak at 2853 cm^{-1}. Besides, the −O−H and −N−H stretching vibrations triggered the peak at 3359 cm^{-1}.[51,52] FTIR of COF−COOH was consistent with the existing literature, demonstrating the successful synthesis of COF−COOH.[45]

The dispersion state of nanoparticles is crucial for the subsequent construction of PDA coating with rough hierarchical nanostructures, which determines whether the nanoparticles can be uniformly dispersed on the membrane surface. The mixture of COF−COOH in sodium acetate buffers remained well dispersed after 30 min sonication and 2 h standing (Figure 1c), and there was no obvious change after standing for 6 h (Figure S2). It is speculated that COF−COOH exhibits excellent dispersibility due to its hydrophilicity as it has been previously reported that imparting hydrophilicity to nanomaterials can significantly improve the dispersibility.[44]

https://doi.org/10.1021/acsami.2c13402
ACS Appl. Mater. Interfaces 2022, 14, 45880−45892

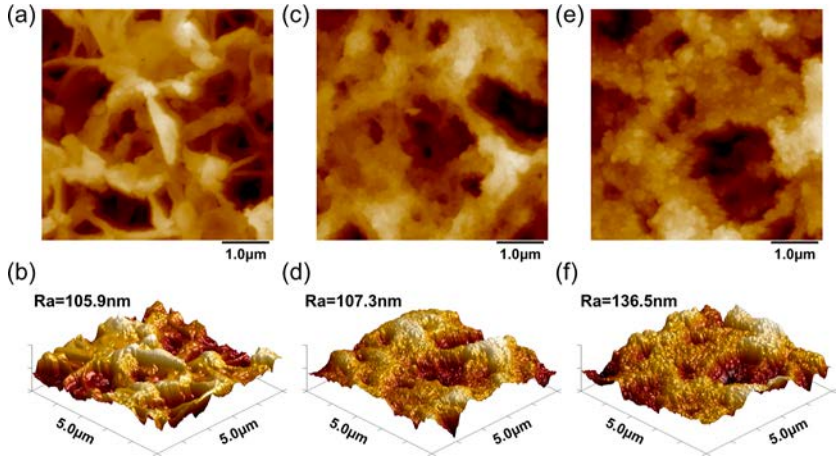

Figure 3. AFM images of (a,b) pristine PVDF membrane, (c,d) COF_0/DA_2-2, and (e,f) $COF_{0.2}/DA_2$-2.

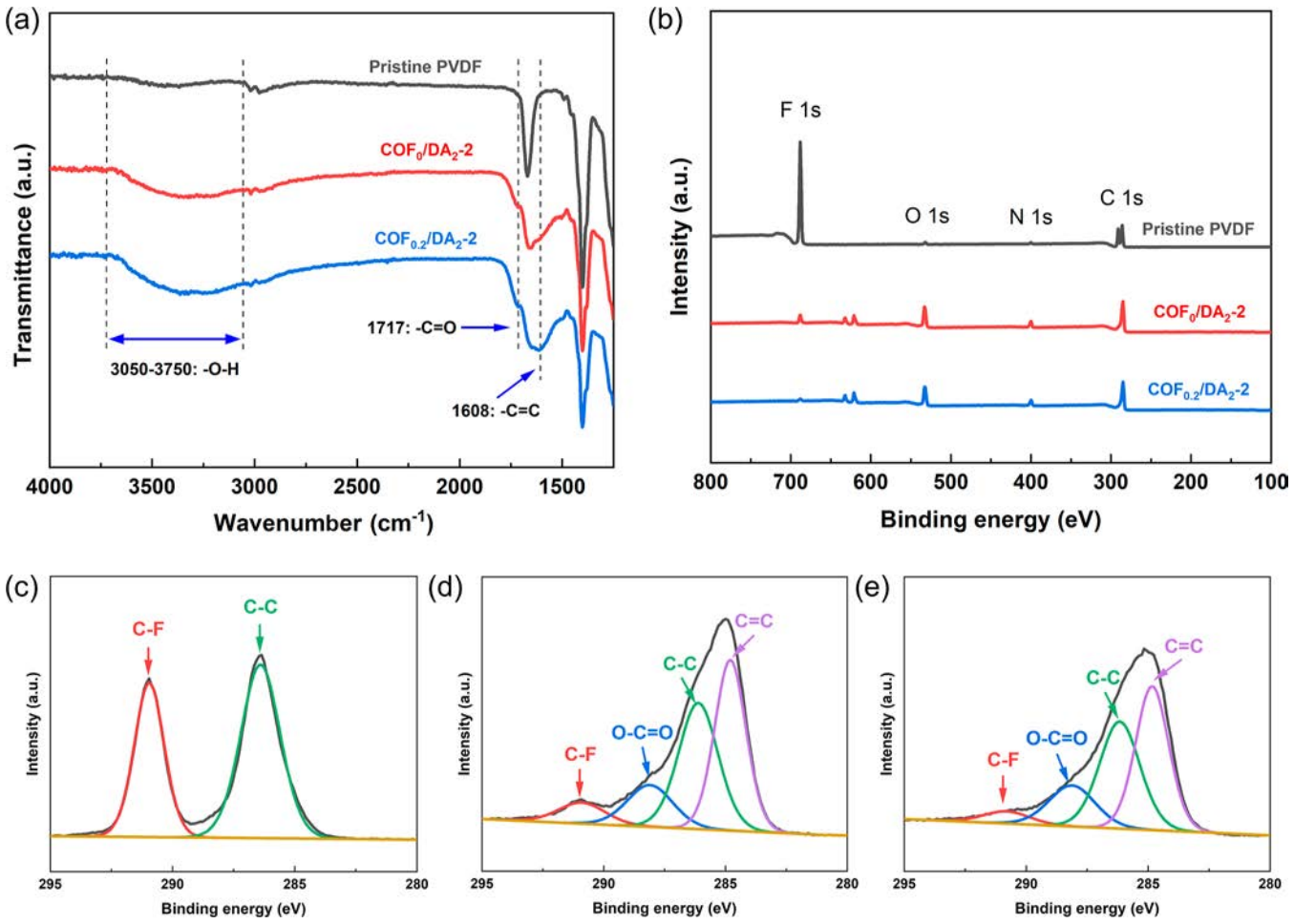

Figure 4. (a) ATR−FTIR spectra and (b) XPS survey spectra of pristine PVDF, COF_0/DA_2-2, and $COF_{0.2}/DA_2$-2. (c−e) High-resolution spectra of C 1s of pristine PVDF membrane, COF_0/DA_2-2, and $COF_{0.2}/DA_2$-2, respectively.

3.2. Surface Morphology and Chemistry of Membranes. Both the surface morphology and chemical composition influence the wettability and oil resistance of oil−water separation membranes.[29] The SEM images of membranes are conducted in Figure 2. The smooth surface of the pristine PVDF membrane with a clear porous structure can be observed (Figure 2a,b). As shown in Figure 2c,d, numerous homogeneous PDA nanoparticles with a size of 35 nm were attached to the internal pore channels and surface of COF_0/DA_2-2. With the incorporation of COF−COOH nanoparticles during the DA oxidation process, an obvious rough hierarchical nanostructure was constructed on the surface as well as pore channels of $COF_{0.2}/DA_2$-2 (Figure 2e,f). COF−COOH with an average particle size of 70 nm and PDA nanoparticles with a mean size of 35 nm were uniformly distributed on the pore channels and surface due to the high interfacial compatibility. Moreover, the

https://doi.org/10.1021/acsami.2c13402
ACS Appl. Mater. Interfaces 2022, 14, 45880−45892

modified membrane also became rougher, and the average roughness (R_a) of the pristine PVDF membrane, COF_0/DA_2-2, and $COF_{0.2}/DA_2$-2 was 105.9, 107.3, and 136.5 nm, respectively (Figure 3). The hydrophilic coating with rough hierarchical nanostructures can capture large amounts of water and form a stable hydration layer to prevent oil contamination.

ATR−FTIR analysis was applied to investigate the surface chemical compositions of membranes (Figure 4a). Compared with the pristine PVDF membrane, COF_0/DA_2-2 and $COF_{0.2}/DA_2$-2 both exhibited two emerging peaks at 1608 and 3050−3750 cm^{-1}, which were attributed to −C═C and −O−H stretching vibrations, respectively.[18,53] Additionally, the modified membranes both showed an extra absorption peak at 1717 cm^{-1} representing −C═O in carboxyl groups.[50] The oxidation of DA by $NaIO_4$ in acidic conditions led to the formation of carboxyl groups on COF_0/DA_2-2,[49] while carboxyl groups of $COF_{0.2}/DA_2$-2 were supplemented by COF−COOH on the basis of DA oxidation process.

XPS analysis was employed to deeply analyze the membrane surface chemistry. As shown in Figure 4b and Table 1, pristine PVDF membrane almost showed peaks of only C and F elements. However, the F 1s peak of COF_0/DA_2-2 and $COF_{0.2}/DA_2$-2 decreased or even disappeared and a new O 1s peak appeared, mainly from catechol, quinone, and carboxyl groups. Moreover, the O/F ratio of $COF_{0.2}/DA_2$-2 (9.28) was found much higher than those of COF_0/DA_2-2 (3.60) and pristine PVDF membrane (0.01), indicating that PDA coating combined with COF−COOH was deposited on the membrane. The high-resolution C 1s spectra of $COF_{0.2}/DA_2$-2 are shown in Figure 4c−e. The peaks at around 284.8, 286.2, 288.4, and 290.8 eV represented −C═C, −C−C, −O−C═O, and −C−F in order.[54] As listed in Table 2, $COF_{0.2}/DA_2$-2 exhibited the highest proportion of −O−C═O group reaching 16.95%, indicating that abundant carboxyl groups were introduced onto the membrane surface. The XPS results are consistent with previous ATR−FTIR conclusions.

Table 1. Elemental Compositions of Different Membranes

	composition (%)				
membrane	C	N	O	F	O/F ratio
pristine PVDF	51.08	0.17	0.48	48.27	0.01
COF_0/DA_2-2	67.36	7.80	19.44	5.40	3.60
$COF_{0.2}/DA_2$-2	68.43	8.45	20.88	2.25	9.28

Table 2. Components of C Element on Pristine PVDF, COF_0/DA_2-2, and $COF_{0.2}/DA_2$-2

	composition (%)			
membrane	−C−F	−O−C═O	−C−C	−C═C
pristine PVDF	40.18		59.82	
COF_0/DA_2-2	7.49	14.41	37.64	40.46
$COF_{0.2}/DA_2$-2	4.86	16.95	36.85	41.34

The surface zeta potential of the membrane also reflected the presence of abundant carboxyl groups. Pristine PVDF membrane showed electronegative properties when it was immersed into water.[18,21] The oxidation of DA by $NaIO_4$ and the accompanying doping of COF−COOH can introduce more abundant carboxyl groups, which were expected to generate more negative charges on the membrane surface. As predicted, $COF_{0.2}/DA_2$-2 exhibited the most negative charge with a surface zeta potential of −34.65 mV (Figure S3). The electrostatic repulsion occurring between the membrane surface and the negatively charged oil droplets can reduce membrane fouling.[44] Lower negative potential of the membrane surface would be more beneficial to elevating the selectivity of oil−water separation.

3.3. Optimization of the Modification Conditions. SDS-stabilized diesel-in-water emulsion was prepared and employed to optimize the modification conditions by filtration. Figure 5a shows the permeate flux of different membranes in which the flux of the pristine PVDF membrane is zero because of its strong hydrophobicity, so its filtering ability was not compared and discussed subsequently. Besides, it was found that the additional amount of COF−COOH displays a significant effect on penetrability. Membrane penetrability first increased and then decreased with the increase of COF−COOH when the coating time was set at 2 h, and $COF_{0.2}/DA_2$-2 exhibited the most attractive flux (897.38 L m^{-2} h^{-1} bar^{-1}) of all. This could be explained by the formation of hierarchical nanostructures. The membrane hydrophilicity was further strengthened due to the increase of surface roughness.[55−57] When the addition of COF−COOH continued to increase, the excessively rough membrane surface provided sufficient sites for small size oil droplets to weaken the antifouling property. Furthermore, the immoderate amounts of nanoparticles hindered the PDA deposition, which affected the modification process to a certain extent and weakened the hydrophilicity, resulting in a decline in flux. This interpretation could also be verified by the WCAs of different membranes (Figure 5b) and by the color of the membrane surface (Figure S4).

The optimization of coating time was also carried out to enhance the penetrability of the membrane. When the addition of COF−COOH was fixed at 0.2 mg/mL, the membrane penetrability was improved significantly with the gradual increase of coating time and decreased slightly after reaching the peak at 2 h (Figure 5c), which means that the membrane hydrophilic modification has been fully completed at 2 h. When the coating time was further extended, the excessive deposition of nanoparticles resulted in a loss of flux, which was reflected by the continuous increase in the weight gain percent of these modified membranes (Figure 5d). The reasons for the optimal coating time of 2 h were further analyzed by observing the surface and cross-sectional morphologies of the membranes with different coating times (0.5−3 h). With the increase of coating time, the rough hierarchical nanostructures gradually emerged on the membrane surface (Figure S5), and the hydrophilic nanoparticles also constantly extended to the internal pore channels of the membrane (Figure S6). At the coating time of 2 h, the membrane interior was covered by numerous nanoparticles, and the membrane exhibited optimal hydrophilicity. Then, the membrane became denser resulting in a decrease in flux due to the continuous deposition of nanoparticles. Hence, $COF_{0.2}/DA_2$-2 (COF−COOH addition: 0.2 mg/mL; coating time: 2 h) exhibited the best penetrability for filtering diesel-in-water emulsion and was regarded as the optimal membrane to further investigate.

3.4. Wettability and Separation Performance of Membranes. The factors such as pore size distribution, surface roughness, and inner hydrophilicity of membranes greatly affect the wettability.[20,58] The membrane surface wettability was assessed by WCA and UOCA tests. The membrane dynamic WCA trends are shown in Figure 6a; the WCA of pristine PVDF remained at 123° for 20 s because of its high hydrophobicity.

https://doi.org/10.1021/acsami.2c13402
ACS Appl. Mater. Interfaces 2022, 14, 45880−45892

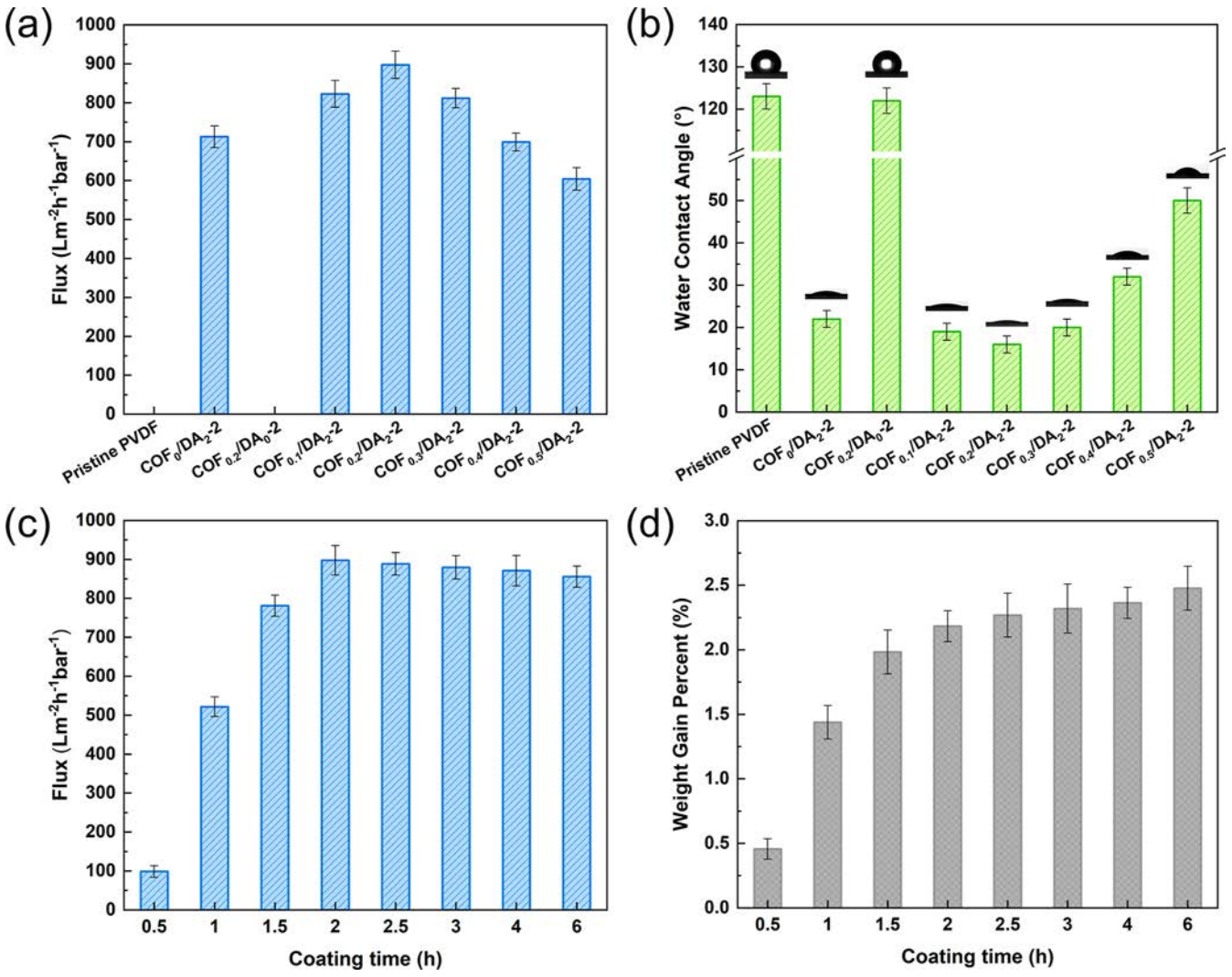

Figure 5. (a) Permeate flux and (b) WCA of pristine membrane and membranes modified by soaking solutions of various COF−COOH amounts (at a fixed coating time of 2 h). (c) Permeate flux and (d) relative weight gain percent of membranes treated by soaking solutions of different coating times (at a fixed COF−COOH amount of 0.2 mg/mL).

Meanwhile, $COF_{0.2}/DA_0$-2 modified only by 0.2 mg/mL COF−COOH showed no WCA change compared with the pristine PVDF membrane. $COF_{0.2}/DA_0$-2 also showed the same zero flux as the pristine PVDF membrane (Figure 5a). The above results indicate that COF−COOH cannot be loaded onto the PVDF membrane without the condition of external factors. After DA chemical oxidation coating, the hydrophilicity of COF_0/DA_2-2 was greatly enhanced with a gradual decrease in WCA from 22 to 0° in 15 s. In addition, after adding 0.2 mg/mL COF−COOH nanoparticles on the basis of COF_0/DA_2-2, the hydrophilicity of $COF_{0.2}/DA_2$-2 was further improved and the WCA rapidly decreased from 15 to 0° within 10 s.

The UOCAs of pristine PVDF membrane, COF_0/DA_2-2, $COF_{0.2}/DA_0$-2, and $COF_{0.2}/DA_2$-2 were measured with the selected oil phase of DCM. As shown in Figure 6b, the UOCA of $COF_{0.2}/DA_2$-2 exhibited a satisfactory result (reaching 162°) with an enormous improvement compared to pristine PVDF membrane (132°). In Figure 6c, the UOCAs of $COF_{0.2}/DA_2$-2 for diesel, kerosene, soybean oil, *n*-hexane, and PE are 163, 160, 164, 161, and 165°, respectively. The excellent underwater superoleophobicity exhibited by $COF_{0.2}/DA_2$-2 was attributed to the rough hierarchical nanostructures (Figure 6d). This structure contributed to improving the wettability and obtaining a thicker and more stable hydration layer. Therefore, $COF_{0.2}/DA_2$-2 with excellent superhydrophilicity and underwater superoleophobicity is expected to be applied to the efficient separation of oil-in-water emulsions.

Besides diesel oil, other oils like kerosene, soybean oil, *n*-hexane, and PE were used to obtain various SDS-stabilized emulsions. Since these oil-in-water emulsions widely exist in real-life environment, using them to evaluate membrane separation performance is of great reference value. As shown in Figure 7a, the fluxes of $COF_{0.2}/DA_2$-2 toward various emulsions followed the sequence of PE (1843.48 L m^{-2} h^{-1} bar^{-1}) > *n*-hexane (1765.29 L m^{-2} h^{-1} bar^{-1}) > diesel (897.38 L m^{-2} h^{-1} bar^{-1}) > soybean oil (795.17 L m^{-2} h^{-1} bar^{-1}) > kerosene (768.59 L m^{-2} h^{-1} bar^{-1}). Meanwhile, the corresponding oil rejection ratio was 98.2, 98.4, 98.9, 99.1, and 99.2% respectively, showing an opposite trend to the flux. In addition, the images of the feed and filtrate of diesel-in-water emulsion were also observed by optical microscopy (Figure 7b); oil droplets with an average size of 2 μm were found in the feed image, while no oil droplets were found in the filtrate image. Hence, $COF_{0.2}/DA_2$-2 exhibits an excellent oil rejection effect,

https://doi.org/10.1021/acsami.2c13402
ACS Appl. Mater. Interfaces 2022, 14, 45880−45892

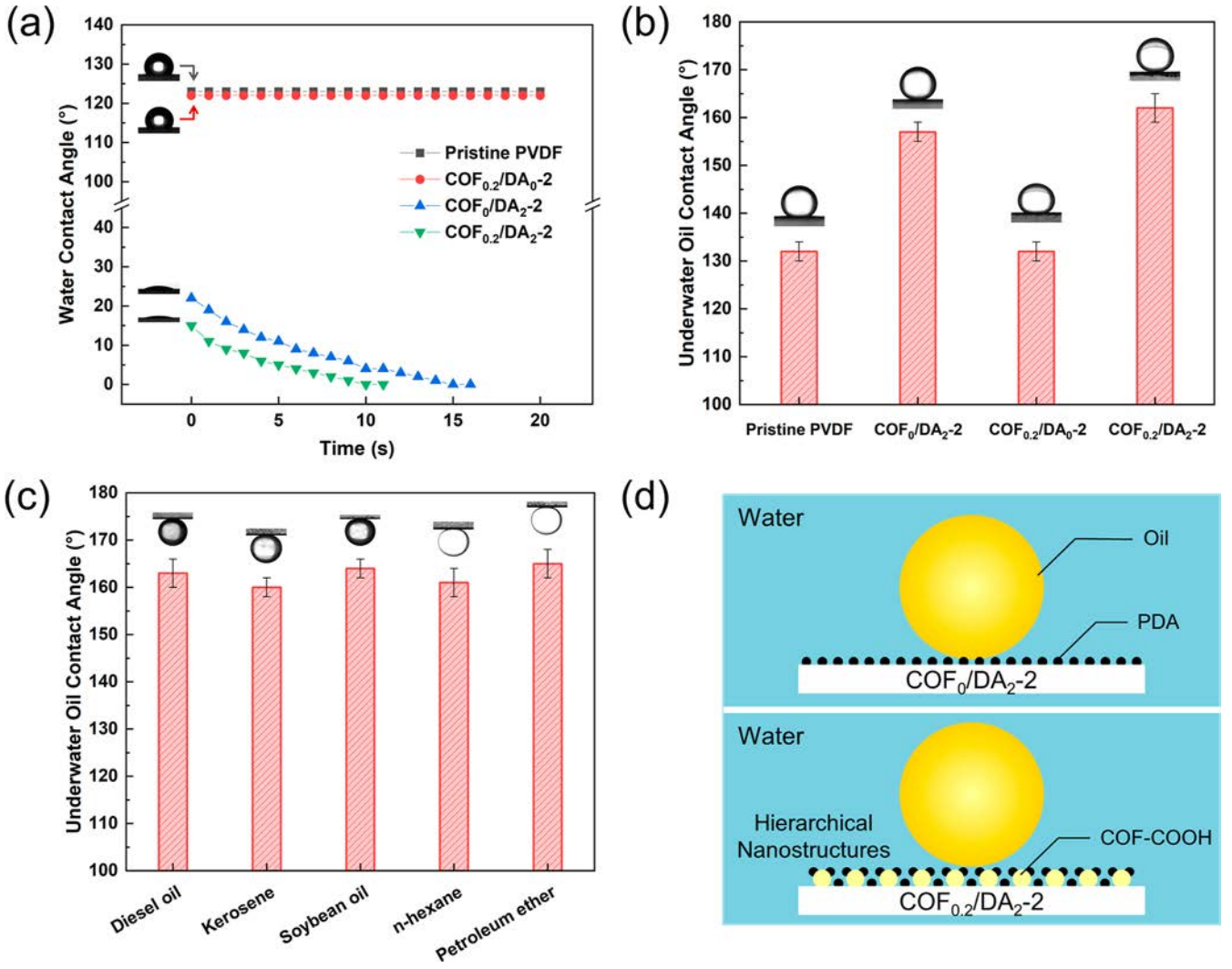

Figure 6. (a) Dynamic WCA and (b) UOCA of pristine PVDF, COF_0/DA_2-2, $COF_{0.2}/DA_0$-2, and $COF_{0.2}/DA_2$-2. (c) UOCAs of $COF_{0.2}/DA_2$-2 using five types of oils. (d) Schematic illustration of an underwater oil droplet on COF_0/DA_2-2 and $COF_{0.2}/DA_2$-2.

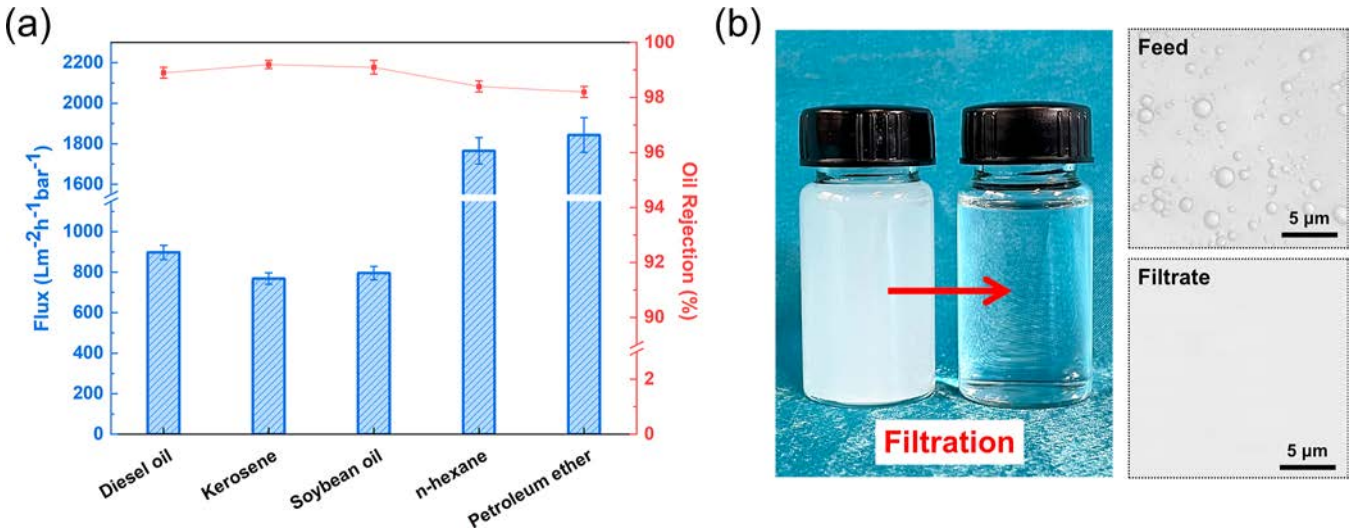

Figure 7. (a) Permeate flux and oil rejection ratio of $COF_{0.2}/DA_2$-2 for five types of SDS-stabilized oil-in-water emulsions. (b) Photograph of the filtration result and microscopic images of the feed and the filtrate.

indicating that it can be effectively devoted to the separation of oil-in-water emulsions. Moreover, the separation performance of the modified membrane for real oily wastewater samples was also investigated. The flux and oil rejection ratio of $COF_{0.2}/DA_2$-

https://doi.org/10.1021/acsami.2c13402
ACS Appl. Mater. Interfaces 2022, 14, 45880−45892

Table 3. Comparison of Performance of the Modified Membrane for Oil-In-Water Emulsions Separation with Other Literature

materials	WCA (°)	flux (L m^{-2} h^{-1} bar^{-1})	R (%)	references
DA/TiO_2/PVDF (0.22 μm)	26.9	424 (diesel)	99.52	29
DA/SiO_2/PVDF (~2 μm)	18 ± 2	572 (dichloroethane)		30
TA/ZIF-8/PVDF (0.22 μm)	21	3726 (pump)	98.9	32
EGCG/Ag/PVDF (0.1 μm)	41 ± 2	1470 (soybean)	95.4	14
TA/GO/TiO_2/PVDF (~0.5 μm)	52	243.11 (*n*-hexadecane)	98.52	55
TA/Ag/PVDF (0.1 μm)	19	1431 (kerosene)	98.41	59
TA/β-FeOOH/PVDF (0.22 μm)	0	645 (soybean)	99.1	60
DA/COF−COOH/PVDF (0.1 μm)	15	897.38 (diesel)	98.9	this work

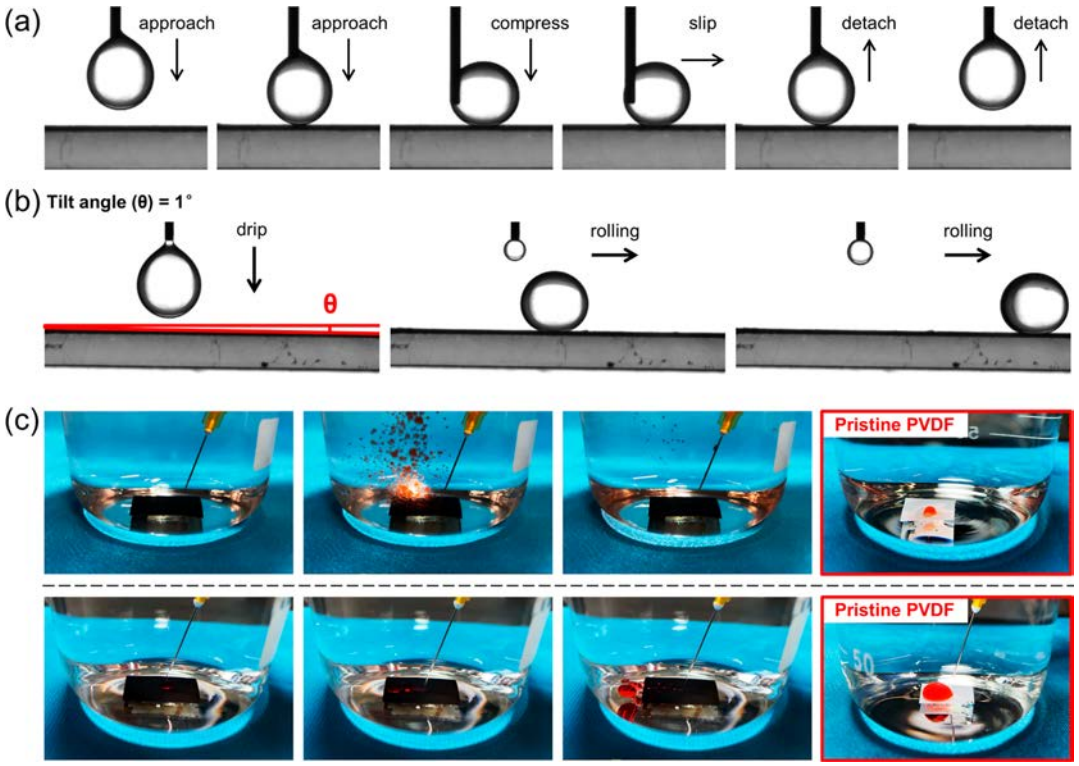

Figure 8. (a) Dynamic underwater DCM-adhesion experiment on $COF_{0.2}/DA_2$-2. (b) Rolling contact test of DCM on $COF_{0.2}/DA_2$-2. (c) Images recording the excellent antifouling property of $COF_{0.2}/DA_2$-2; *n*-hexane (top four images) and DCM (bottom four images) were injected onto the membrane by a syringe, respectively.

2 is presented in Figure S7, it still displayed an excellent oil interception ability except for some reduction in flux. By comparing the liquid pictures before and after filtration, it was found that the filtrate became clear (Figure S8). Therefore, the membrane developed in this work also exhibits attractive potential for practical applications.

Besides, we compared the separation performance of $COF_{0.2}/DA_2$-2 with nanoparticle-decorated membranes reported in other similar modification works. As summarized in Table 3, the modified membrane developed in this work displayed attractive hydrophilicity and great separation performance, demonstrating its favorable competitive advantages in oil-in-water emulsion separation.

3.5. Antifouling Property and Stability of Membrane. Moreover, to assess the anti-oil fouling of $COF_{0.2}/DA_2$-2, underwater oil adhesion tests were carried out. As shown in Figure 8a, a drop of DCM was brought onto the surface of membrane and squeezed and then lifted completely. During the entire test, it can be found that the oil droplet did not detach from the needle and did not deform under a larger force (Video S1). Besides, the dropped DCM droplets rolled away quickly without any sticking when the membrane tilt angle was as low as 1° (Figure 8b and Video S2), which further verified its splendid underwater superoleophobicity. In addition, a small amount of kerosene (dyed red) and DCM (dyed red) were sprayed onto the surface of $COF_{0.2}/DA_2$-2 by a syringe. As shown in Figure 8c, kerosene rebounded from the surface of $COF_{0.2}/DA_2$-2 and then floated up onto the surface of the water driven by buoyancy, and DCM droplets gathered to form bigger oil droplets after touching the membrane surface and then quickly slid away. During the whole experiment, oil droplets did not adhere to $COF_{0.2}/DA_2$-2 at all. However, pristine PVDF membrane was easily adhered by oil droplets under a similar test. All above results demonstrated that $COF_{0.2}/DA_2$-2 possessed exceptional antifouling property, which was due to the robust hydration layer formed by hierarchical nanostructures and the electrostatic repulsion caused by carboxyl groups.

To further evaluate the reusability and antifouling property of $COF_{0.2}/DA_2$-2, five-cycle filtration experiments were carried out. As shown in Figure 9, the formation of an oil cake layer by transmembrane pressure resulted in a sharp decrease of flux at the beginning of each filtration process[61−65] and then decreased

https://doi.org/10.1021/acsami.2c13402
ACS Appl. Mater. Interfaces 2022, 14, 45880−45892

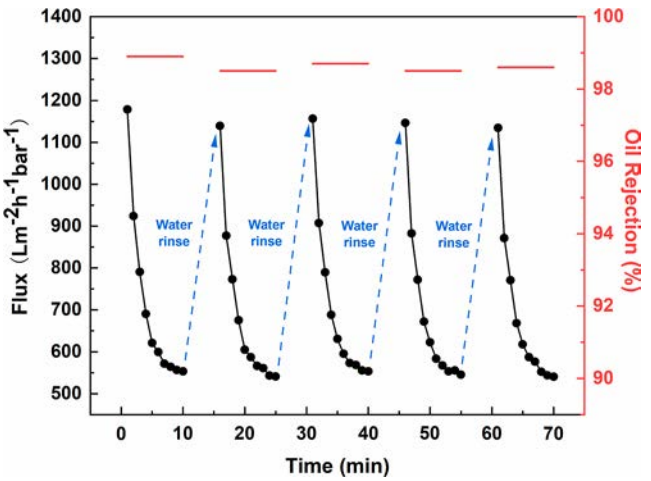

Figure 9. Permeate flux and rejection of $COF_{0.2}/DA_2$-2 in five cycles of separation of SDS-stabilized diesel-in-water emulsion.

relatively slowly. Nevertheless, after the previous filtration, the residual oil on the membrane surface was washed away by DI water and the flux was almost recovered to the initial level in the next filtration. Since the oil rejection ratios of five-cycle filtration experiments remained above 98%, the separation efficiency was not significantly reduced. Besides, after filtering the diesel-in-water emulsion for five cycles, $COF_{0.2}/DA_2$-2 still exhibited a pure water FRR of 98.31% (J_{w0} = 2779.62 L m^{-2} h^{-1} bar^{-1}, J_w = 2732.64 L m^{-2} h^{-1} bar^{-1}), indicating that its pure water permeability could basically restore to the initial level. The above results demonstrated that $COF_{0.2}/DA_2$-2 exhibits a favorable antifouling property and satisfactory reusability.

$COF_{0.2}/DA_2$-2 was soaked in neutral (pH = 7), strong acid (pH = 2), and strong basic (pH = 12) solutions separately for 12 h to evaluate its chemical stability. As shown in Figure 10a,b, $COF_{0.2}/DA_2$-2 still maintained satisfactory superhydrophilicity and underwater superoleophobicity after being treated with different pH solutions from the results of WCAs and UOCAs, which indicated its favorable chemical stability. Moreover, the coating stability of $COF_{0.2}/DA_2$-2 was tested by sonication in an ultrasonic machine. As shown in Figure 10c, after physical stress treatment, both the WCAs and UOCAs of $COF_{0.2}/DA_2$-2 did not change significantly. The favorable stability of $COF_{0.2}/DA_2$-2 may benefit from two reasons. On the one hand, the strong oxidation of $NaIO_4$ in a slightly acidic environment enhanced the oxidation degree of DA, and the layer-by-layer stacking of PDA obtained by further oxidation intensified the cross-linking strength with the membrane.[49,66] On the other hand, the excellent compatibility matching between COF−COOH and PDA also improved the coating bonding strength.

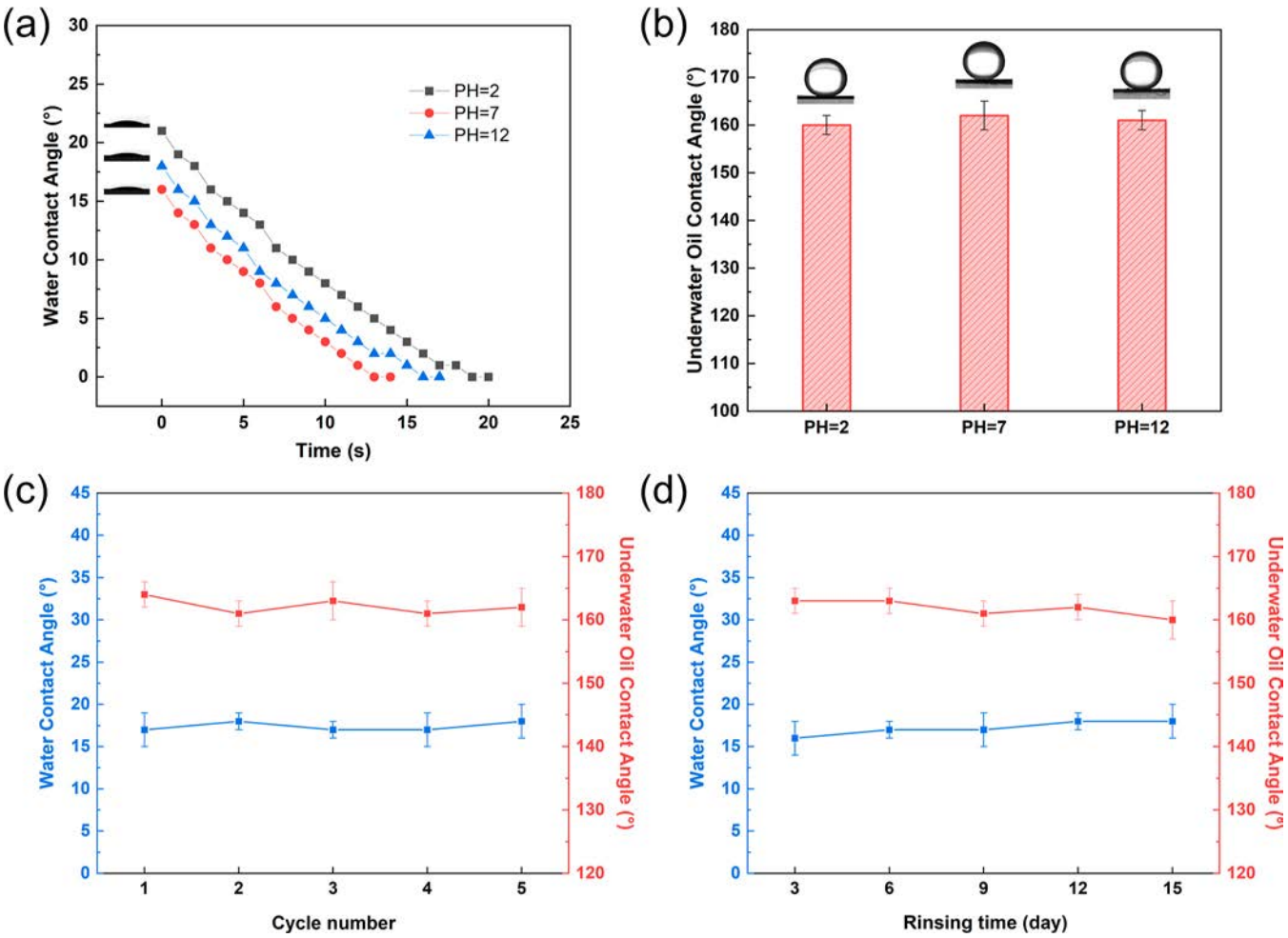

Figure 10. (a) Dynamic WCAs and (b) UOCAs of $COF_{0.2}/DA_2$-2 after being treated with harsh pH solutions. (c) UOCAs and initial WCAs of $COF_{0.2}/DA_2$-2 during five-cycle sonication. (d) UOCAs and initial WCAs of $COF_{0.2}/DA_2$-2 after being rinsed with DI water for different days.

https://doi.org/10.1021/acsami.2c13402
ACS Appl. Mater. Interfaces 2022, 14, 45880−45892

To further assess the long-term stability of $COF_{0.2}/DA_2$-2, long-term rinsing experiments were performed. The modified membranes could maintain stable superhydrophilicity and underwater superoleophobicity under long-term immersion in water, which was a necessary condition to ensure sustainable and efficient operation of oil−water separation. Both the WCAs and UOCAs of $COF_{0.2}/DA_2$-2 remained stable after being scoured by DI water for 15 days (Figure 10d), proving its favorable long-term stability.

4. CONCLUSIONS

In this work, a hierarchical assembly strategy was explored to realize the uniform construction of COF−COOH on the PVDF membrane surface and pore channels. The membrane penetrability and surface wettability were effectively optimized by changing the amount of COF−COOH and coating time. The optimally modified membrane (COF−COOH addition: 0.2 mg/mL; coating time: 2 h) exhibited admirable superhydrophilicity and underwater superoleophobicity. The membrane maintained a high flux (the maximum flux of PE-in-water emulsion reaches 1843.48 L m^{-2} h^{-1} bar^{-1}) and an ultrahigh oil rejection ratio (exceeded 98% for all emulsions). Moreover, the membrane revealed splendid antifouling property with the FRR of 98.31%, satisfactory reusability, and impregnable stability. In conclusion, this study would bring a new reference for the development of superwettable membranes in the field of oil-in-water emulsion separation.

■ ASSOCIATED CONTENT

Supporting Information

The Supporting Information is available free of charge at https://pubs.acs.org/doi/10.1021/acsami.2c13402.

Detailed modification conditions and abbreviations of the membranes, schematic diagram of the cross-flow filtration apparatus, dispersion of COF−COOH in sodium acetate buffers, zeta potentials of the membranes, photographs of the membranes, surface and cross-sectional SEM images of the membranes obtained under different coating times, permeate flux and oil rejection ratio of $COF_{0.2}/DA_2$-2 in filtering real samples, and pictures of real sample and filtrate (PDF)

Dynamic underwater DCM-adhesion experiment (MP4)

Rolling contact test of DCM (MP4)

■ AUTHOR INFORMATION

Corresponding Author

Luhong Zhang − *School of Chemical Engineering and Technology, Tianjin University, Tianjin 300072, People's Republic of China;* orcid.org/0000-0002-7073-4793; Phone: +86 22 27400199; Email: zhanglvh@tju.edu.cn

Authors

Qi Liang − *School of Chemical Engineering and Technology, Tianjin University, Tianjin 300072, People's Republic of China*

Bin Jiang − *School of Chemical Engineering and Technology, Tianjin University, Tianjin 300072, People's Republic of China*

Na Yang − *School of Chemical Engineering and Technology, Tianjin University, Tianjin 300072, People's Republic of China;* orcid.org/0000-0003-4888-5971

Longfei Zhang − *School of Chemical Engineering and Technology, Tianjin University, Tianjin 300072, People's Republic of China*

Yongli Sun − *School of Chemical Engineering and Technology, Tianjin University, Tianjin 300072, People's Republic of China*

Complete contact information is available at: https://pubs.acs.org/10.1021/acsami.2c13402

Author Contributions

Q.L. and B.J. have contributed equally. All authors have given approval to the final version of the manuscript.

Notes

The authors declare no competing financial interest.

■ ACKNOWLEDGMENTS

We are grateful for the financial support from the National Key R&D Program of China (2017YFB0602702-02). The authors also thank Shiyanjia Lab (www.shiyanjia.com) for the support of XPS test.

■ REFERENCES

(1) Cheng, X.; Ye, Y.; Li, Z.; Chen, X.; Bai, Q.; Wang, K.; Zhang, Y.; Drioli, E.; Ma, J. Constructing Environmental-Friendly "Oil-Diode" Janus Membrane for Oil/Water Separation. *ACS Nano* **2022**, *16*, 4684−4692.

(2) Zheng, W.; Huang, J.; Li, S.; Ge, M.; Teng, L.; Chen, Z.; Lai, Y. Advanced Materials with Special Wettability toward Intelligent Oily Wastewater Remediation. *ACS Appl. Mater. Interfaces* **2020**, *13*, 67−87.

(3) Zhao, Y.; Zhang, Y.; Li, F.; Bai, Y.; Pan, Y.; Ma, J.; Zhang, S.; Shao, L. Ultra-robust superwetting hierarchical membranes constructed by coordination complex networks for oily water treatment. *J. Membr. Sci.* **2021**, *627*, 119234.

(4) Li, Y. J.; Yuan, D.; Geng, Q.; Yang, X.; Wu, H. Z.; Xie, Y. Z.; Wang, L. M.; Ning, X.; Ming, J. F. MOF-Embedded Bifunctional Composite Nanofiber Membranes with a Tunable Hierarchical Structure for High-Efficiency $PM_{0.3}$ Purification and Oil/Water Separation. *ACS Appl. Mater. Interfaces* **2021**, *13*, 39831−39843.

(5) Saththasivam, J.; Loganathan, K.; Sarp, S. An overview of oil−water separation using gas flotation systems. *Chemosphere* **2016**, *144*, 671−680.

(6) Elhemmali, A.; Anwar, S.; Zhang, Y. H.; Shirokoff, J. A comparison of oil-water separation by gravity and electrolysis separation process. *Sep. Sci. Technol.* **2021**, *56*, 359−373.

(7) Zhao, C.; Zhou, J.; Yan, Y.; Yang, L.; Xing, G.; Li, H.; Wu, P.; Wang, M.; Zheng, H. Application of coagulation/flocculation in oily wastewater treatment: A review. *Sci. Total Environ.* **2021**, *765*, 142795.

(8) Doshi, B.; Repo, E.; Heiskanen, J. P.; Sirviö, J. A.; Sillanpää, M. Sodium salt of oleoyl carboxymethyl chitosan: A sustainable adsorbent in the oil spill treatment. *J. Cleaner Prod.* **2018**, *170*, 339−350.

(9) Krebs, T.; Schroën, C. G. P. H.; Boom, R. M. Separation kinetics of an oil-in-water emulsion under enhanced gravity. *Chem. Eng. Sci.* **2012**, *71*, 118−125.

(10) Pintor, A. M. A.; Vilar, V. J. P.; Botelho, C. M. S.; Boaventura, R. A. R. Oil and grease removal from wastewaters: Sorption treatment as an alternative to state-of-the-art technologies. A critical review. *Chem. Eng. J.* **2016**, *297*, 229−255.

(11) Wang, M. K.; Zhang, Z. Z.; Wang, Y. L.; Zhao, X.; Men, X. H.; Yang, M. M. Ultrafast Fabrication of Metal-Organic Framework-Functionalized Superwetting Membrane for Multichannel Oil/Water Separation and Floating Oil Collection. *ACS Appl. Mater. Interfaces* **2020**, *12*, 25512−25520.

(12) Chu, Z.; Feng, Y.; Seeger, S. Oil/Water Separation with Selective Superantiwetting/Superwetting Surface Materials. *Angew. Chem., Int. Ed.* **2015**, *54*, 2328−2338.

(13) Gu, J. C.; Ji, L. T.; Xiao, P.; Zhang, C.; Li, J.; Yan, L. K.; Chen, T. Recent Progress in Superhydrophilic Carbon-Based Composite Membranes for Oil/Water Emulsion Separation. *ACS Appl. Mater. Interfaces* **2021**, *13*, 36679−36696.
(14) Zhang, N.; Yang, N.; Zhang, L.; Jiang, B.; Sun, Y.; Ma, J.; Cheng, K.; Peng, F. Facile hydrophilic modification of PVDF membrane with Ag/EGCG decorated micro/nanostructural surface for efficient oil-in-water emulsion separation. *Chem. Eng. J.* **2020**, *402*, 126200.
(15) Zhan, H.; Peng, N.; Lei, X.; Huang, Y.; Li, D.; Tao, R.; Chang, C. UV-induced self-cleanable TiO_2/nanocellulose membrane for selective separation of oil/water emulsion. *Carbohydr. Polym.* **2018**, *201*, 464−470.
(16) Kang, G.-d.; Cao, Y.-m. Application and modification of poly(vinylidene fluoride) (PVDF) membranes—A review. *J. Membr. Sci.* **2014**, *463*, 145−165.
(17) Otitoju, T. A.; Ahmad, A. L.; Ooi, B. S. Polyvinylidene fluoride (PVDF) membrane for oil rejection from oily wastewater: A performance review. *J. Water Process. Eng.* **2016**, *14*, 41−59.
(18) Jiang, B.; Cheng, K.; Zhang, N.; Yang, N.; Zhang, L.; Sun, Y. One-step modification of PVDF membrane with tannin-inspired highly hydrophilic and underwater superoleophobic coating for effective oil-in-water emulsion separation. *Sep. Purif. Technol.* **2021**, *255*, 117724.
(19) Cui, J.; Zhou, Z.; Xie, A.; Wang, Q.; Liu, S.; Lang, J.; Li, C.; Yan, Y.; Dai, J. Facile preparation of grass-like structured NiCo-LDH/PVDF composite membrane for efficient oil−water emulsion separation. *J. Membr. Sci.* **2019**, *573*, 226−233.
(20) Zhao, Y.; Yang, X.; Yan, L.; Bai, Y.; Li, S.; Sorokin, P.; Shao, L. Biomimetic nanoparticle-engineered superwettable membranes for efficient oil/water separation. *J. Membr. Sci.* **2021**, *618*, 118525.
(21) Sun, Y.; Zong, Y.; Yang, N.; Zhang, N.; Jiang, B.; Zhang, L.; Xiao, X. Surface hydrophilic modification of PVDF membranes based on tannin and zwitterionic substance towards effective oil-in-water emulsion separation. *Sep. Purif. Technol.* **2020**, *234*, 116015.
(22) Yang, X.; Yuan, L.; Zhao, Y.; Yan, L.; Bai, Y.; Ma, J.; Li, S.; Sorokin, P.; Shao, L. Mussel-inspired structure evolution customizing membrane interface hydrophilization. *J. Membr. Sci.* **2020**, *612*, 118471.
(23) Wang, Z.; Ji, S.; He, F.; Cao, M.; Peng, S.; Li, Y. One-step transformation of highly hydrophobic membranes into superhydrophilic and underwater superoleophobic ones for high-efficiency separation of oil-in-water emulsions. *J. Mater. Chem. A* **2018**, *6*, 3391−3396.
(24) Miller, D. J.; Dreyer, D. R.; Bielawski, C. W.; Paul, D. R.; Freeman, B. D. Surface Modification of Water Purification Membranes. *Angew. Chem., Int. Ed.* **2017**, *56*, 4662−4711.
(25) Zhu, Y. Z.; Xie, W.; Zhang, F.; Xing, T. L.; Jin, J. Superhydrophilic In-Situ-Cross-Linked Zwitterionic Polyelectrolyte/PVDF-Blend Membrane for Highly Efficient Oil/Water Emulsion Separation. *ACS Appl. Mater. Interfaces* **2017**, *9*, 9603−9613.
(26) Lee, H.; Dellatore, S. M.; Miller, W. M.; Messersmith, P. B. Mussel-Inspired Surface Chemistry for Multifunctional Coatings. *Science* **2007**, *318*, 426−430.
(27) Huang, Q.; Chen, J.; Liu, M.; Huang, H.; Zhang, X.; Wei, Y. Polydopamine-based functional materials and their applications in energy, environmental, and catalytic fields: State-of-the-art review. *Chem. Eng. J.* **2020**, *387*, 124019.
(28) Tao, M.; Xue, L.; Liu, F.; Jiang, L. An Intelligent Superwetting PVDF Membrane Showing Switchable Transport Performance for Oil/Water Separation. *Adv. Mater.* **2014**, *26*, 2943−2948.
(29) Shi, H.; He, Y.; Pan, Y.; Di, H.; Zeng, G.; Zhang, L.; Zhang, C. A modified mussel-inspired method to fabricate TiO_2 decorated superhydrophilic PVDF membrane for oil/water separation. *J. Membr. Sci.* **2016**, *506*, 60−70.
(30) Cui, J.; Zhou, Z.; Xie, A.; Meng, M.; Cui, Y.; Liu, S.; Lu, J.; Zhou, S.; Yan, Y.; Dong, H. Bio-inspired fabrication of superhydrophilic nanocomposite membrane based on surface modification of SiO_2 anchored by polydopamine towards effective oil-water emulsions separation. *Sep. Purif. Technol.* **2019**, *209*, 434−442.
(31) Huang, Y.; Jiao, Y.; Chen, T.; Gong, Y.; Wang, S.; Liu, Y.; Sholl, D. S.; Walton, K. S. Tuning the Wettability of Metal-Organic Frameworks via Defect Engineering for Efficient Oil/Water Separation. *ACS Appl. Mater. Interfaces* **2020**, *12*, 34413−34422.
(32) Wang, R. X.; Zhao, X. T.; Jia, N.; Cheng, L. J.; Liu, L. F.; Gao, C. J. Superwetting Oil/Water Separation Membrane Constructed from In Situ Assembled Metal-Phenolic Networks and Metal-Organic Frameworks. *ACS Appl. Mater. Interfaces* **2020**, *12*, 10000−10008.
(33) Zhang, Y. Q.; Guo, J.; Han, G.; Bai, Y. P.; Ge, Q. C.; Ma, J.; Lau, C. H.; Shao, L. Molecularly soldered covalent organic frameworks for ultrafast precision sieving. *Sci. Adv.* **2021**, *7*, No. eabe8706.
(34) Wang, Z.; Zhang, S.; Chen, Y.; Zhang, Z.; Ma, S. Covalent organic frameworks for separation applications. *Chem. Soc. Rev.* **2020**, *49*, 708−735.
(35) Wang, R.; Shi, X.; Zhang, Z.; Xiao, A.; Sun, S.-P.; Cui, Z.; Wang, Y. Unidirectional diffusion synthesis of covalent organic frameworks (COFs) on polymeric substrates for dye separation. *J. Membr. Sci.* **2019**, *586*, 274−280.
(36) Shen, J.; Yuan, J.; Shi, B.; You, X.; Ding, R.; Zhang, T.; Zhang, Y.; Deng, Y.; Guan, J.; Long, M.; Zheng, Y.; Zhang, R.; Wu, H.; Jiang, Z. Homointerface covalent organic framework membranes for efficient desalination. *J. Mater. Chem. A* **2021**, *9*, 23178−23187.
(37) Jiang, Y.; Liu, C.; Li, Y.; Huang, A. Stainless-steel-net-supported superhydrophobic COF coating for oil/water separation. *J. Membr. Sci.* **2019**, *587*, 117177.
(38) Chen, L.; Du, J.; Zhou, W.; Shen, H.; Tan, L.; Zhou, C.; Dong, L. Microwave-Assisted Solvothermal Synthesis of Covalent Organic Frameworks (COFs) with Stable Superhydrophobicity for Oil/Water Separation. *Chem.—Asian J.* **2020**, *15*, 3421−3427.
(39) Liu, Y.; Li, W.; Yuan, C.; Jia, L.; Liu, Y.; Huang, A.; Cui, Y. Two-Dimensional Fluorinated Covalent Organic Frameworks with Tunable Hydrophobicity for Ultrafast Oil-Water Separation. *Angew. Chem., Int. Ed.* **2022**, *61*, No. e202113348.
(40) Liu, Y.; Lyu, Q.; Wang, Z.; Sun, Y.; Li, C.; Sun, S.; Lin, L.-C.; Hu, S. A flame-retardant post-synthetically functionalized COF sponge as absorbent for spilled oil recovery. *J. Mater. Sci.* **2021**, *56*, 13031−13042.
(41) Chen, A.; Guo, H.; Zhou, J.; Li, Y.; He, X.; Chen, L.; Zhang, Y. Polyacrylonitrile Nanofibers Coated with Covalent Organic Frameworks for Oil/Water Separation. *ACS Appl. Nano Mater.* **2022**, *5*, 3925−3936.
(42) Wang, H.; Wang, M.; Wang, Y.; Wang, J.; Men, X.; Zhang, Z.; Singh, V. Synergistic effects of COF and GO on high flux oil/water separation performance of superhydrophobic composites. *Sep. Purif. Technol.* **2021**, *276*, 119268.
(43) Li, J.; Yang, X.; Bai, C.; Tian, Y.; Li, B.; Zhang, S.; Yang, X.; Ding, S.; Xia, C.; Tan, X.; Ma, L.; Li, S. A novel benzimidazole-functionalized 2-D COF material: Synthesis and application as a selective solid-phase extractant for separation of uranium. *J. Colloid Interface Sci.* **2015**, *437*, 211−218.
(44) Cao, J.; Su, Y.; Liu, Y.; Guan, J.; He, M.; Zhang, R.; Jiang, Z. Self-assembled MOF membranes with underwater superoleophobicity for oil/water separation. *J. Membr. Sci.* **2018**, *566*, 268−277.
(45) Xu, L.; Yang, T.; Li, M.; Chang, J.; Xu, J. Thin-film nanocomposite membrane doped with carboxylated covalent organic frameworks for efficient forward osmosis desalination. *J. Membr. Sci.* **2020**, *610*, 118111.
(46) Zhang, N.; Song, X.; Jiang, H.; Tang, C. Y. Advanced thin-film nanocomposite membranes embedded with organic-based nanomaterials for water and organic solvent purification: A review. *Sep. Purif. Technol.* **2021**, *269*, 118719.
(47) Cheng, K.; Zhang, N.; Yang, N.; Hou, S.; Ma, J.; Zhang, L.; Sun, Y.; Jiang, B. Rapid and robust modification of PVDF ultrafiltration membranes with enhanced permselectivity, antifouling and antibacterial performance. *Sep. Purif. Technol.* **2021**, *262*, 118316.
(48) Wang, Z.; Yang, H.-C.; He, F.; Peng, S.; Li, Y.; Shao, L.; Darling, S. B. Mussel-Inspired Surface Engineering for Water-Remediation Materials. *Matter* **2019**, *1*, 115−155.
(49) Luo, C.; Liu, Q. Oxidant-Induced High-Efficient Mussel-Inspired Modification on PVDF Membrane with Superhydrophilicity and Underwater Superoleophobicity Characteristics for Oil/Water Separation. *ACS Appl. Mater. Interfaces* **2017**, *9*, 8297−8307.

https://doi.org/10.1021/acsami.2c13402
ACS Appl. Mater. Interfaces 2022, 14, 45880−45892

(50) Ponzio, F.; Barthès, J.; Bour, J.; Michel, M.; Bertani, P.; Hemmerlé, J.; d'Ischia, M.; Ball, V. Oxidant Control of Polydopamine Surface Chemistry in Acids: A Mechanism-Based Entry to Superhydrophilic-Superoleophobic Coatings. *Chem. Mater.* **2016**, *28*, 4697−4705.
(51) López-Ballester, E.; Doménech-Carbó, M. T.; Gimeno-Adelantado, J. V.; Bosch-Reig, F. Study by FT-IR spectroscopy of ageing of adhesives used in restoration of archaeological glass objects. *J. Mol. Struct.* **1999**, *482-483*, 525−531.
(52) Tang, C. Y. Y.; Kwon, Y. N.; Leckie, J. O. Effect of membrane chemistry and coating layer on physiochemical properties of thin film composite polyamide RO and NF membranes I. FTIR and XPS characterization of polyamide and coating layer chemistry. *Desalination* **2009**, *242*, 149−167.
(53) Jiang, J.; Zhu, L.; Zhu, L.; Zhang, H.; Zhu, B.; Xu, Y. Antifouling and Antimicrobial Polymer Membranes Based on Bioinspired Polydopamine and Strong Hydrogen-Bonded Poly(N-vinyl pyrrolidone). *ACS Appl. Mater. Interfaces* **2013**, *5*, 12895−12904.
(54) Chen, Y.; Liu, Q. Oxidant-induced plant phenol surface chemistry for multifunctional coatings: Mechanism and potential applications. *J. Membr. Sci.* **2019**, *570-571*, 176−183.
(55) Du, C.; Liu, G.; Qu, Z.; Wang, W.; Yu, D. GO/TiO_2-decorated electrospun polyvinylidene fluoride membrane prepared based on metal-polyphenol coordination network for oil−water separation and desalination. *J. Mater. Sci.* **2022**, *57*, 3452−3467.
(56) Ao, C.; Hu, R.; Zhao, J.; Zhang, X.; Li, Q.; Xia, T.; Zhang, W.; Lu, C. Reusable, salt-tolerant and superhydrophilic cellulose hydrogel-coated mesh for efficient gravity-driven oil/water separation. *Chem. Eng. J.* **2018**, *338*, 271−277.
(57) Wang, M.; Peng, M.; Zhu, J.; Li, Y. D.; Zeng, J. B. Mussel-inspired chitosan modified superhydrophilic and underwater superoleophobic cotton fabric for efficient oil/water separation. *Carbohydr. Polym.* **2020**, *244*, 116449.
(58) Huang, S.; Ras, R. H. A.; Tian, X. Antifouling membranes for oily wastewater treatment: Interplay between wetting and membrane fouling. *Curr. Opin. Colloid Interface Sci.* **2018**, *36*, 90−109.
(59) Zhang, Y.; Duan, X.; Tan, B.; Jiang, Y.; Wang, Y.; Qi, T. PVDF microfiltration membranes modified with AgNPs/tannic acid for efficient separation of oil and water emulsions. *Colloids Surf., A* **2022**, *644*, 128844.
(60) Xie, A.; Cui, J.; Yang, J.; Chen, Y.; Dai, J.; Lang, J.; Li, C.; Yan, Y. Photo-Fenton self-cleaning membranes with robust flux recovery for an efficient oil/water emulsion separation. *J. Mater. Chem. A* **2019**, *7*, 8491−8502.
(61) Venault, A.; Chen, L.-A.; Maggay, I. V.; Marie Yap Ang, M. B.; Chang, H.-Y.; Tang, S.-H.; Wang, D.-M.; Chou, C.-J.; Bouyer, D.; Quémener, D.; Lee, K.-R.; Chang, Y. Simultaneous amphiphilic polymer synthesis and membrane functionalization for oil/water separation. *J. Membr. Sci.* **2020**, *604*, 118069.
(62) Wang, Z.; Jiang, X.; Cheng, X.; Lau, C. H.; Shao, L. Mussel-Inspired Hybrid Coatings that Transform Membrane Hydrophobicity into High Hydrophilicity and Underwater Superoleophobicity for Oil-in-Water Emulsion Separation. *ACS Appl. Mater. Interfaces* **2015**, *7*, 9534−9545.
(63) Yan, L. L.; Yang, X. B.; Zhao, Y. Y.; Wu, Y. D.; Motlhaletsi Moutloali, R. M.; Mamba, B. B.; Sorokin, P.; Shao, L. Bio-inspired mineral-hydrogel hybrid coating on hydrophobic PVDF membrane boosting oil/water emulsion separation. *Sep. Purif. Technol.* **2022**, *285*, 120383.
(64) Huang, Y.; Li, H.; Wang, L.; Qiao, Y.; Tang, C.; Jung, C.; Yoon, Y.; Li, S.; Yu, M. Ultrafiltration Membranes with Structure-Optimized Graphene-Oxide Coatings for Antifouling Oil/Water Separation. *Adv. Mater. Interfaces* **2015**, *2*, 1400433.
(65) Zuo, C. J.; Wang, L. B.; Tong, Y. J.; Shi, L. J.; Ding, W. L.; Li, W. X. Co-deposition of pyrogallol/polyethyleneimine on polymer membranes for highly efficient treatment of oil-in-water emulsion. *Sep. Purif. Technol.* **2021**, *267*, 118660.
(66) Wei, H. L.; Ren, J.; Han, B.; Xu, L.; Han, L. L.; Jia, L. Y. Stability of polydopamine and poly(DOPA) melanin-like films on the surface of polymer membranes under strongly acidic and alkaline conditions. *Colloids Surf., B* **2013**, *110*, 22−28.

https://doi.org/10.1021/acsami.2c13402
ACS Appl. Mater. Interfaces 2022, 14, 45880−45892